Journal of Materials Chemistry A

Accepted Manuscript

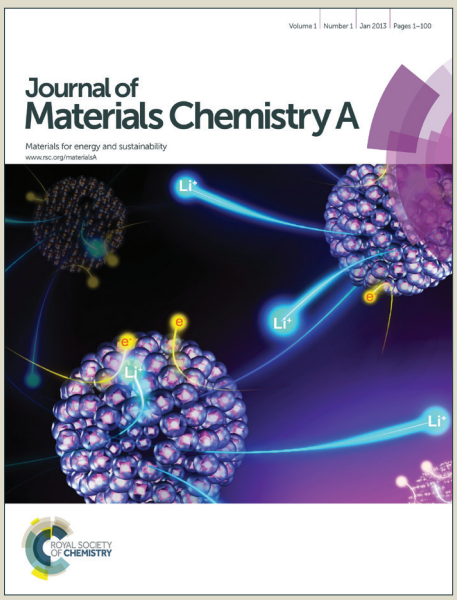

ROYAL SOCIETY OF CHEMISTRY

www.rsc.org/materialsA

Journal Name

RSCPublishing

ARTICLE

Hybrid ionogel electrolytes for high temperature lithium batteries

Cite this: DOI: 10.1039/x0xx00000x

Jin Hong Lee,[a,b]‡ Albert S. Lee,[a]‡ Jong-Chan Lee,[b] Soon Man Hong,[a,c] Seung Sang Hwang[a,c] and Chong Min Koo*[a,c]

Received 00th January 2012,
Accepted 00th January 2012

DOI: 10.1039/x0xx00000x

www.rsc.org/

Hybrid ionogels fabricated with 1M LiTFSI in N-butyl-N-methylpyrrolidinium bis(trifluoromethylsulfonyl)imide (BMPTFSI) crosslinked with a ladder-like structured poly(methacryloxypropyl)silsesquioxane (LPMASQ) were investigated as high temperature ionogel electrolytes for lithium ion batteries. In addition to the exceeding low crosslinker concentration (~2 wt %) required to completely solidify the ionic liquids, which provided high ionic conductivities comparable to the liquid state ionic liquid, these hybrid ionogels exhibited superior thermal stabilities (> 400 °C). Rigorous lithium ion battery cells fabricated with these hybrid ionogels revealed excellent cell performance at various C-rates at a variety of temperatures, comparable with those of neat liquid electrolyte. Moreover, these hybrid ionogels exhibited excellent cycling performance during 50 cycles at 90 °C, sustaining over 98% coulombic efficiency. Highly advantageous properties of these hybrid ionogels, such as high ionic conductivity in the gel state, thermal stability, excellent C-rate performance, cyclability and nonflammability offer opportunities for applications as high temperature electrolytes.

Introduction

Ionic liquids have been widely investigated as possible solutions for next generation of electrolytes in electrochemical cells due to their advantageous properties of high ionic conductivity, high electrochemical stability, nonflammability, negligible vapour pressure and high thermal stability.[1,2] Despite these advantages over lithium salt solutions,[3,4] ionic liquid electrolytes still face problems of leakage and low cycling properties, which has proved to be a serious concern for some applications, for instance in fully electronic or hybrid vehicles.[2] To solve the problem of leakage in liquid electrolytes, research of gel polymer electrolytes (GPEs) have been pervasive in electrochemical device applications, such as capacitors and lithium ion batteries.[5–7]

Gel polymer electrolytes can be defined as a class of electrolytes in which the liquid electrolyte is either swollen in polymers or crosslinked through thermally- or photo-initiated processes.[8,9] Extensive reports have detailed the utility of organic polymers as matrix or crosslinkable oligomers/polymers as crosslinking agent.[8–10] Furthermore, GPEs can be classified depending on the type of solidified liquid electrolyte solution, as ionogels are GPEs composed of solidified ionic liquids.[11] Many ionogels have been fabricated using a variety of structural support materials, including polymers, colloidal particles, carbon nanotubes and crosslinkable small organic molecules.[12] While these approaches have been proved to be extremely useful for the fabrication of gels and films, considerable amounts of matrix or crosslinking agent compared with the liquid electrolyte needed for the solidification of ionic liquid have had major depreciating effects on the electrochemical devices performances.[12] Therefore, minimal use of crosslinking agent, while maintaining nonflowing, solid-like behaviour, has remained a challenge for optimal electrochemical devices.

Inorganic-organic hybrid materials, such as silicon-oxide based materials, have also been garnered great interest as support matrix for ionogels for their favourable properties; for instance, thermal stability, electrochemical stability and facile processing.[13–22] Several studies have detailed the electrochemical studies and Li battery applications with chemically modified siloxanes, such as commercially available $[RSiO_{1.5}]_n$ polysilsesquioxane-based ORMOCERS,[23] or $[SiO_2]_n$ silica-based materials, as ionogel support matrix.[13–17] These approaches have either entailed the use of organic crosslinking functionalities or the *in situ* sol–gel gelation of ionic liquids using hydrolytic or non-hydrolytic sol–gel processes.[13–17] Notable studies by Vioux[15–17] and Panzer[13] groups have detailed the *in situ* gelation of ionic liquids to yield ionogels with tunable flexibility. However, the fabrication of these ionogels *in situ* sol–gel reactions may have a number of long-term problems in the solid state, as uncondensed silanol groups may produce water molecules through secondary condensations. Additionally, organic acids, such as formic acid, which are used for catalyzing the sol–gel hydrolysis-

condensation rearrangements, may not be completely removed *in vacuo*, thus remaining as impurities. The long times (5 days~2 weeks) needed to solidify the ionic liquid *in situ* is also a process unfavourable for the industrial applications.[14]

Another class of hybrid gel polymer electrolytes include composites of oxides particles. Functional silane-coated oxide-based nanoparticles,[24–27] which have been rigorously investigated by the Archer group, and 'soggy sand' electrolytes, which have been investigated by Bhattacharyya[28–30] are representative examples of such composites. Surface modification of oxide-based nanoparticles coated with functional silanes (*e.g.*, ionic liquid groups, oligo-polyethylene oxide groups, and single ion conducting groups) provides excellent electrochemical stability and mechanical robustness compared with the neat liquid electrolytes.[24] Soggy sands electrolytes, which comprise of oxide particles dispersed in nonaqueous liquid solutions, have also been widely investigated as structural supporting agents to solidify the liquid electrolytes.[28–31] However, for application in lithium ion battery, these hybrid gel polymer electrolytes should provide impeccable dispersion in liquid electrolytes to achieve well-defined homogeneous composites. Mechanical properties of these materials are still too low for such an application. These are issues that still need to be addressed and thoroughly investigated for practical lithium ion battery applications.

Polysilsesquioxanes (PSQs) with chemical formula of $[RSiO_{1.5}]_n$ are a class of inorganic-organic hybrid materials in which a silicon oxide network structure is equipped with an organic functionality.[32] There are three structural classes of PSQs, random-branched network, polyhedral cage and ladder-like polymers. Although polyhedral cage structures, also known as polyhedral oligomeric silsesquioxanes (POSS), have been used as crosslinker or additive,[33–36] their general low solubility[37] has limited their applications as composites with ionic liquids. In addition, as mentioned above, ionogels fabricated from random-branched structural PSQ-modified silica particles suffer from remnant silanol groups that will condense to form water molecules over time, making their applications in Li batteries practically infeasible.

Ladder-like structured polysilsesquioxanes (LPSQs) are a unique class of silsesquioxanes in which the siloxane bond is double stranded and the organic functional groups are unidirectionally positioned to the siloxane bonds.[37–42] These materials exhibit enhanced solubility and superior thermal stability because of the imperceptible amount of silanol groups, which only reside at the polymer end groups.[37–42]The acid resistance and insensitivity to thermal history characters can also be said to be highly attractive merits of these materials as polymer electrolytes. The polymeric nature of these materials allows for the introduction of several hundreds of organic moieties per polymer chain for fast and easy curing process.[37,38] Recently, our research group developed a facile, one-pot synthesis of LPSQs using a base-catalyzed system.[37–40] The products of the synthesis were fully condensed high molecular weight LPSQs. Compared with the above approaches towards hybrid gel polymer electrolytes, these materials are highly soluble in nonaqueous electrolytes and ionic liquids, leading to high homogeneity, whereas they need only a small amount of gelator.

In this study, we synthesized a novel ladder-structured poly(methacryloxypropyl)silsesquioxane (LPMASQ) following our method and used it as a crosslinker for an ionic liquid electrolyte, 1M LiTFSI in *N*-butyl-*N*-methylpyrrolidinium bis(trifluoromethylsulfonyl)imide (BMPTFSI). Thermal crosslinking of the methacryl moieties of LPMASQ resulted in homogenous, non-leaking hybrid ionogels. The thermal, mechanical and flame retardant properties of these inorganic-organic hybrid gel polymer electrolytes were examined and Li battery cells were fabricated to test their application as thermally stable and high performance ionogels.

Experimental

Materials

3-methacryloxypropyltrimethoxysilane (Shin-Etsu, 98%) and ethyl acetate (J.T. Baker, HPLC grade) were distilled over CaH_2 prior to use. Potassium carbonate (Daejung) was dried at 40 °C. THF (J.T. Baker, HPLC grade) was distilled over sodium. Azobisisobutyronitrile (Daejung) was recrystallised from methanol. Lithium bis(trifluoromethylsulfonyl)imide (LiTFSI) (Aldrich, 99.9%, battery grade), 1-methylpyrrolidine (Aldrich, 98%), 1-iodobutane (Aldrich, 99%) and all other solvents were used as received.

Synthesis of LPMASQ

LPMASQ was synthesized following a known literature procedure.[37–40] In a typical experiment, potassium carbonate, K_2CO_3 (0.04 g, 0.29 mmol) was dissolved in deionised H_2O (4.8 mL, 0.27 mol) and 8 g of THF was added. To this solution, 3-methacryloxypropyltrimethoxysilane (19.9 mL, 0.08 mol) was added dropwise under nitrogen flow. The solution was magnetically stirred for 10 days when the molecular weight reached its maximum value. After partial evaporation of THF, the resinous material was dissolved in dichloromethane and extracted several times with water. Collection of the organic layers followed by drying of the organic layer over anhydrous magnesium sulphate and evaporation of the solvent under reduced pressure yielded a transparent liquid with medium viscosity (15.2 g, 95% crude yield). LPMASQ was found to have excellent solubility in the majority of organic solvents.

^{1}H NMR ($CDCl_3$) (δ, ppm):
(0.48–0.78, $SiCH_2CH_2CH_2OCOCCH_2CH_3$),
(1.5–1.75, $SiCH_2CH_2CH_2OCOCCH_2CH_3$),
(3.9–4.1, $SiCH_2CH_2CH_2OCOCCH_2CH_3$),
(5.4, 5.9, $SiCH_2CH_2CH_2OCOCCH_2CH_3$),
(1.75–1.85, $SiCH_2CH_2CH_2OCOCCH_2CH_3$),
^{13}C NMR ($CDCl_3$) (δ, ppm):
(7.6–10.3, $SiCH_2CH_2CH_2OCOCCH_2CH_3$),
(17.5–18.5, $SiCH_2CH_2CH_2OCOCCH_2CH_3$),
(21.2–22.4, $SiCH_2CH_2CH_2OCOCCH_2CH_3$),
(65.4–66.8, $SiCH_2CH_2CH_2OCOCCH_2CH_3$),
(124.4–126.1, $SiCH_2CH_2CH_2OCOCCH_2CH_3$),

(135.5–136.9, $SiCH_2CH_2CH_2OCOCCH_2CH_3$), (166.6–168.6, $SiCH_2CH_2CH_2OCOCCH_2CH_3$), ^{29}Si NMR (ppm): –65 to –68 ppm, M_w = 26,000 g mol^{-1}, M_w/M_n = 2.1

Synthesis of *N*-butyl-*N*-methylpyrrolidinium bis(trifluoromethylsulfonyl)imide

Synthesis of BMPTFSI was performed following literature procedure.[43] In a dry 500 mL round-bottom flask, stoichiometric amounts of 1-methylpyrrolidine (50 g, 0.59 mol) and 1-iodobutane (108 g, 0.59 mol) in 250 mL of ethyl acetate were magnetically stirred at room temperature for 24 h. The product was repeatedly washed with ethyl acetate and filtered until pure white salt of BMPI was obtained. BMPI was then dissolved in deionized water and mixed with a stoichiometric amount of LiTFSI dissolved in deionized water. The organic phase was extracted with methylene chloride and subsequently dried at 100 °C for 24 h to remove any residual water. The resulting BMP–TFSI had H_2O content of less than 100 ppm as measured with the Karl Fischer method. The ^{1}H NMR characterization of BMPTFSI is shown in ESI, Fig S1†.

Preparation of hybrid ionogels

In an inert, argon-charged glove, solutions with various amounts of LPMASQ in 1M LiTFSI in BMPTFSI were prepared in glass vial. An amount of 1 wt % (relative to LPMASQ) of AIBN as thermal initiator was added to this solution. After taking the solutions out of the glove box, samples were sonicated and shaken for 10 min or until the solution was homogenous. Then, the samples were directly taken to an oven preset at 70 °C for 3 h. The hybrid ionogels were named as HI-2 and HI-5 for ionogels containing 2 and 5 wt % of LPMASQ, respectively.

Characterisations and measurements

Fourier transform infrared spectra were measured with a Perkin-Elmer FT-IR system Spectrum-GX. Number average molecular weight (M_n) and molecular weight distributions (M_w/M_n) of polymers were measured using JASCO PU-2080 plus SEC system equipped with refractive index detector (RI-2031 plus), UV detector (λ = 254 nm, UV-2075 plus) and Viscotek SLS apparatus using THF as the mobile phase at 40 °C with a flow rate of 1 mL min^{-1}. The samples were separated through four columns (Shodex-GPC KF-802, KF-803, KF-804, KF-805). ^{1}H-NMR and ^{29}Si NMR spectra were recorded in $CDCl_3$ at 25 °C using a Varian Unity INOVA (^{1}H: 300 MHz, ^{29}Si: 59.6 MHz). Thermal gravimetric analysis was carried out with TA instrument (TGA 2950) at heating rate of 10 °C min^{-1} under N_2 atmosphere.

Rheological properties were examined using a rheometer (Advanced Rheometric Expansion System, ARES) instrument with cone-plate geometry (25 mm diameter). All rheological measurements were performed in the linear viscoelastic region under nitrogen atmosphere.

The ionic conductivity was determined using a complex impedance analyzer (Bio-Logics, VMP3) over frequency range from 1 Hz to 1 MHz at AC amplitude of 10 mV. The electrochemical stability of the gel polymer electrolytes was examined using a linear sweep voltammetry system. In the experiments, a stainless steel working electrode was used with lithium metal as both the counter and reference electrodes. The voltage was swept at a scan rate of 1.0 mV s^{-1}. The time evolution dependence of interfacial resistance between the lithium metal and the ionogel was measured through monitoring the AC impedance response over the frequency range from 100 KHz to 10 MHz of the Li/HI-2/Li symmetric cells. Electrochemical measurements of the gel polymer electrolyte were conducted using 2032 coin cells consisting of a separator, Li metal and a $LiFePO_4$ cathode (90 wt % $LiFePO_4$, 5 wt % carbon black, 5 wt % PVDF). All the cells were assembled in argon-charged glove box. After fabrication, the cells with pre-gel solution were subjected to thermal cross-linking for 3 h at 70 °C. The galvanostatic charge-discharge experiments were carried out with voltage range of 2.5–4.2 V using a battery cycler (Wonatech, WBCS3000) at room temperature.

Results and Discussion

Inorganic-organic hybrid ionogel fabrication

The synthesis and characterization of LPMASQ has been previously reported.[37] This facile and mass-producible method for production of highly condensed ladder-like structured polysilsesquioxanes has been proved to be extremely useful for high yield production of LPSQs. The obtained LPMASQ was then dissolved in an ionic liquid solution of 1M LiTFSI in BMPTFSI with various amounts of AIBN as thermal initiator (Scheme 1). Through mild thermal treatment at 70 °C, non-leaking, homogenous hybrid ionogels were able to be easily processed as free-standing gels (Scheme 1, inset). As shown in the right model, we expected the LPMASQ network being formed after crosslinking was loose enough to facilitate high lithium mobility within the LPMASQ network. The obtained hybrid ionogels were HI-2, HI-5 containing 2 and 5 wt % of LPMASQ, respectively.

Scheme 1 Fabrication of hybrid ionogels

Through extensive pre-trials, we observed that LPMASQ was capable of completely solidifying BMPTFSI, even at an exceeding low concentration of 2 wt % (HI-2). As shown in Fig. 1, the peaks assigned to the C=C bonds at 1635 cm^{-1} completely disappeared after curing process, demonstrating that the cross-linking reaction was completed. The inset photograph in Fig. 1 shows that the ionic liquid electrolyte was completely

solidified after thermal curing. Similar to our previous study,[37] we demonstrated that LPMASQ was able to produce mechanically pliant and non-flowing gel polymer electrolytes using only a mere 2 wt % of gelator. This stable formation of homogenous ionogels led us to hypothesize optimal electrochemical performance with these hybrid ionogels.

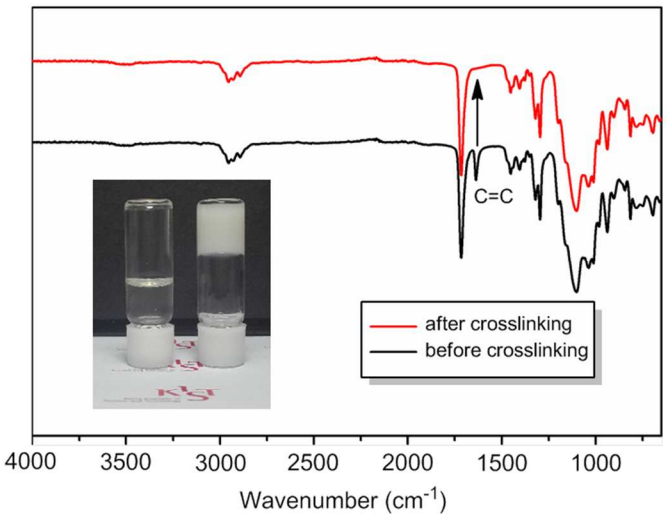

Fig. 1 FTIR spectra of hybrid ionogel HI-5 before and after thermal curing with inset photograph.

Rheological properties of hybrid ionogels

Rheological examinations of gel polymer electrolytes and hybrid ionogels have recently observed as an efficient method to elucidate the mechanical properties of such soft materials.[24–29] Fig. 2a presents the changes of dynamic viscoelastic properties of neat BMPTFSI and hybrid ionogels as a function of angular frequency. For the neat BMPTFSI, the loss modulus G″ was found greater than storage modulus G′. Both dynamic moduli values exhibited power law dependency over the experimental range, which is a typical rheological characteristic of a viscous fluid.[29,30] These results clearly demonstrate the dynamic shift from liquid to solid-like state; predominantly elastic behaviour with only minimal addition of LPMASQ due to the well-developed network structure. Meanwhile, with increasing LPMASQ concentration, the network structure becomes denser, resulting in an increase in the gel rigidity, as evident by the increase in dynamic modulus order. Furthermore, as shown in Fig. 2b, the thermal scanning rheological observation for hybrid ionogel HI-2 showed that storage modulus values were stable as temperatures exceeding 250 °C.

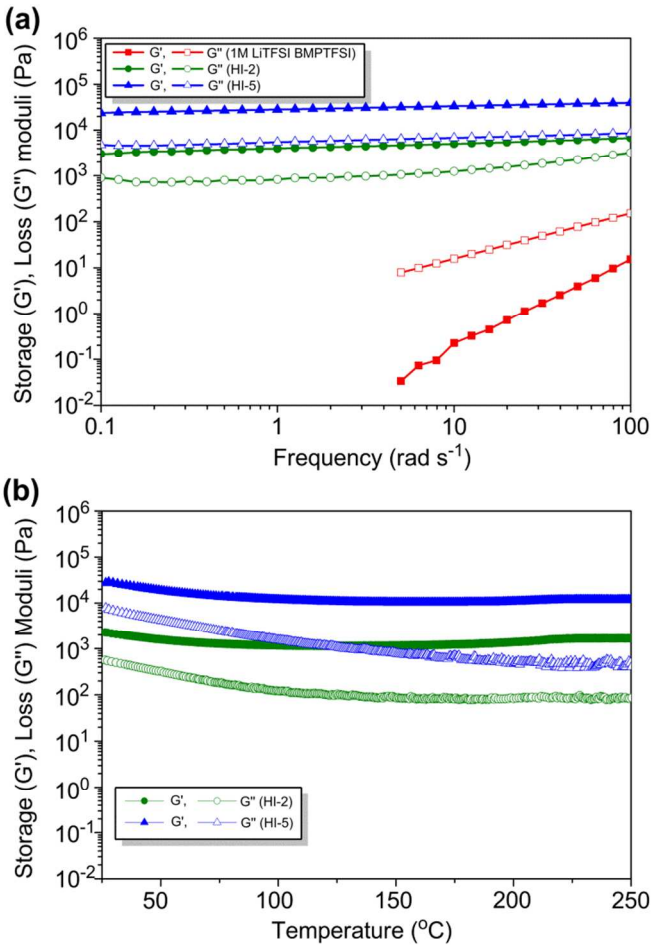

Fig. 2 Rheological properties of hybrid ionogels (a) frequency sweep (b) temperature sweep.

Thermal stability

Thermal stability of electrolytes is a critical requirement for their safety and stability in lithium ion battery applications. The TGA thermograms of LPMASQ, BMPTFSI and two kinds of prepared hybrid ionogels are presented in Fig. 3. As shown, the initial degradation temperature of LPMASQ and BMPTFSI are very similar (~400 °C), but LPMASQ left residual silica at temperatures exceeding 500 °C. The residual mass of the hybrid ionogels at various concentrations also correlated well with the LPMASQ concentration as ionogels with larger LPMASQ concentration gave greater residual mass at 800 °C. Given the exceeding high initial degradation temperature of these hybrid ionogels, it can be said that these materials exhibit superior thermal stability. Moreover, thermal shrinkage tests with the neat ionic liquid compared with HI-2 impregnated polypropylene (PP) separator were conducted at 150 °C for 30 minutes (Fig 3b). As shown, the neat ionic liquid impregnated PP separator showed significant shrinkage, while the HI-2 impregnated PP separator showed exceptionally low thermal shrinkage, indicating that these hybrid ionogels have superior thermal and thermo-mechanical properties for use at elevated temperatures.

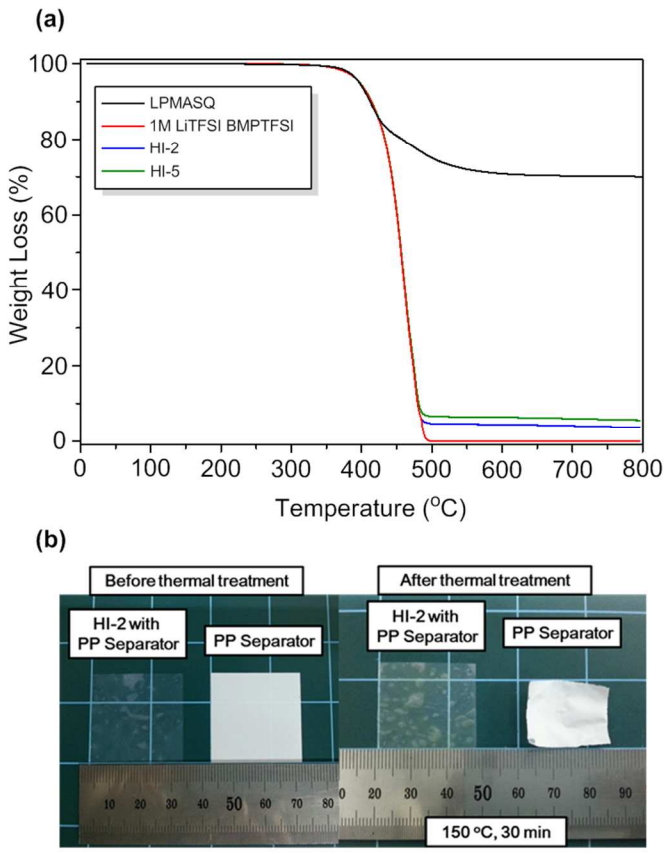

Fig. 3 (a) TGA thermograms of BMPTFSI, LPMASQ, and hybrid ionogels, (b) Thermal shrinkage tests with neat ionic liquid and HI-2 impregnated polypropylene separators

Electrochemical properties of hybrid ionogels

Ionic conductivity. The temperature dependency of ionic conductivity of gel polymer electrolytes produced with various amounts of cross-linker was examined via AC impedance spectroscopy technique. The ionic conductivity (σ) of an electrolyte can be described using the following equation.[36]

$$\sigma(T) = \Sigma\, n \times q \times \mu$$

where n is the number of charge carriers, q is the charge on the charge carrier, and μ is the mobility of charge carriers. Hybrid ionogels fabricated through the gelation of liquid electrolyte can provide good mechanical properties, though at the cost of sacrificing ionic conductivity. The ionic mobility (μ) correlated to the diffusion of ions is hindered when compared with the 1M LiTFSI in BMPTFSI electrolyte due to the formation of a network structure. Furthermore, a decrease in the number of the charge carrier (n) per unit volume of electrolyte, caused by the introduction of the crosslinking agent, is also a contributing factor for the restricted ionic conductivity. A notable advantage of this work is the gelation of ionic liquid with 2 wt % LPMASQ. Due to the minimal amount of gelator content used to fabricate these free-standing hybrid ionogels, high ionic conductivity similar to the neat BMPTFSI was expected. As shown in Fig. 4, a decrease in ionic conductivity was observed for hybrid ionogels with increasing the amounts of LPMASQ. However, the ionic conductivity of HI-2 was observed as 0.79 mS cm^{-1} at 30 °C, which is in close proximity to the ionic conductivity of the neat ionic liquid electrolyte (0.96 mS cm^{-1}). In addition, we plotted the ionic conductivities of a commercially available organic-based crosslinker (ETPTA) utilized in several previous studies.[44] As shown, the high amounts of ETPTA required for full solidification of 1M LiTFSI BMPTFSI led to the drastic decrease in ionic conductivities and subsequent poor cell performance to be discussed later.

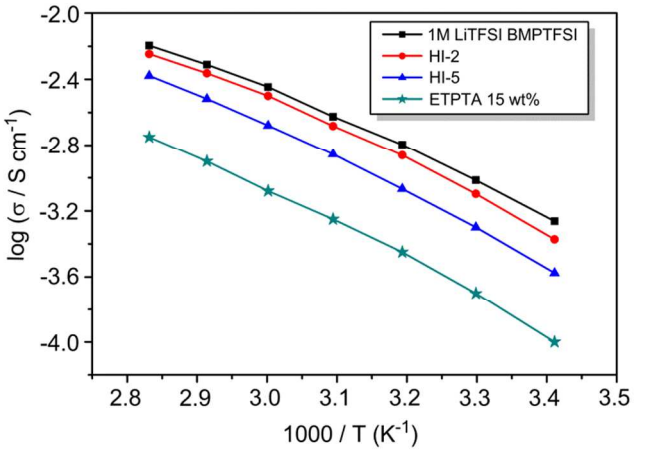

Fig. 4 Temperature dependency of ionic conductivities of hybrid ionogels.

Electrochemical stability. The electrochemical stability of electrolytes over the operating voltage of a lithium-ion battery is also an important requirement for practical battery operation. The linear sweep voltammetry (LSV) measurements were performed in the potential between 3.0 and 7.0 V (V vs. Li/ Li^+) under various temperature conditions. As shown in Fig. 5, upon the voltage sweep, the onset of the oxidation current increase, which is related to the electrochemical oxidative decomposition of electrolyte shifted closer to 5.0 V with increasing temperature. Greater slopes of I-E diagrams were also observed at higher temperatures, indicating that oxidation current depends on the test temperature. However, no significant oxidation current was observed below 5.0 V even at elevated temperatures, demonstrating that obtained gel polymer electrolytes were electrochemically stable up to 5.0 V, which could be applied to high-voltage lithium batteries over a wide temperature range.

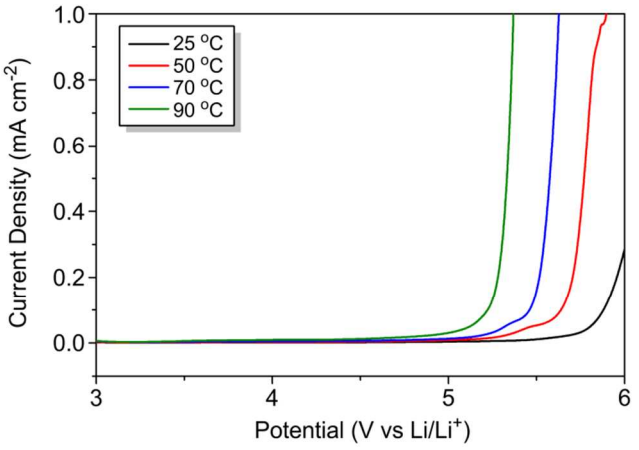

Fig. 5 Linear sweep voltamagrams of hybrid ionogel HI-2 at various temperatures.

Interfacial stability towards the Li metal electrode. To evaluate the compatibility of Li metal electrodes with hybrid ionogels, the interfacial resistance of Li/HI-2/Li test cell was monitored during a period of 25 days. Fig. 6 shows the time evolution of the AC impedance spectra under open-circuit potential conditions. The intercept with the Z_{real} axis at high frequency presents the bulk resistance (R_s), which remained stable and constant with the storage time, confirming the stability of ionogels against the lithium metal. In comparison, the mid-frequency semicircle associated with the interfacial resistance (R_{int}) gradually increased with time until a steady state was reached (ESI, Fig. S2†). Such a response could be explained by the formation of the passivation layer on the lithium metal electrode surface that suppresses continuous electrochemical reactions between the lithium metal electrode and electrolyte, resulting in the stabilization after a few days of storage.[45,46] The electrochemical behaviour of the hybrid ionogel toward lithium metal was further investigated with running a cyclic voltammetry (CV) of a symmetrical Li/HI-2/Li cell. As ESI Fig S3† reveals, the cell exhibited reversible redox process with high coulombic efficiency, and the peak current of CV profile tended to decrease with increase in cycle number. These results also confirm the stabilization at the interface, suggesting that the compatibility of the ionogel towards the lithium metal electrode is sufficient for application in lithium batteries.

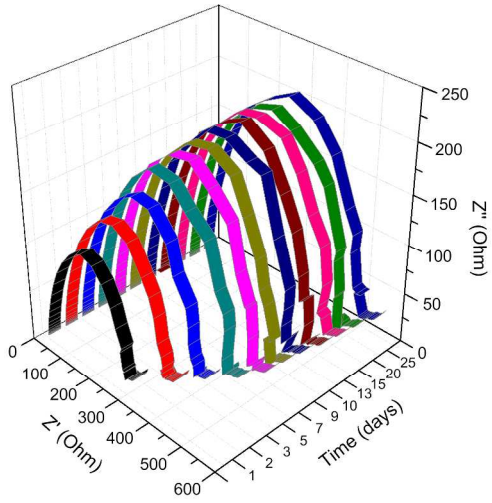

Fig. 6 Nyquist plot of AC impedance for a Li/HI-2/Li cell.

Cell performance. To characterize electrochemical performance of hybrid ionogels, we fabricated coin cells using $LiFePO_4$ as the cathode and metallic lithium counter electrodes assembled with HI-2 (98 wt % of ionic liquid containing 2 wt % LPMASQ). Fig. 7a presents the discharge capacity of the cells at various temperatures. In the examination, the cells were charged at a constant current density of 0.1 C (1 C rate corresponded to a current density of 155.1 mA g^{-1}) and discharged at various current densities in a voltage range of 2.5–4.2 V. As shown, the cells delivered stable discharge capacity upon repeated cycling at various current rates. However, the discharge capacity and voltage of cells gradually decreased when the discharging current density rate increased. This lower discharge capacity is attributed to the increase in cell polarization caused by the poor kinetics at the electrode-electrolyte interface.[47] With increasing temperature, as expected, discharge capacity of cell increased. For instance, in the initial cycle at 50 °C, the discharge capacity with a current density of 0.5 C was 88.3 mAh g^{-1}, whereas cells cycled at 90 °C delivered a greater discharge capacity of 156.2 mAh g^{-1}, which is close to the theoretical discharge capacity of the cathode active material in this potential region (170 mAh g^{-1} for $LiFePO_4$).

Typical discharge profiles of the cell fabricated with HI-2 at various temperatures with 0.1C charge-0.1C discharge are displayed in Fig. 7b. In general, a flat voltage plateau at approximately 3.4 V (vs. Li/Li^+) corresponds to the conversion between $LiFePO_4$ and $FePO_4$.[47,48] A well-defined voltage plateau was observed above 50 °C, whereas the truncated flat voltage region and the voltage drops were observed at 30 °C. These results clearly show that the limited conversion process is mainly due to the low diffusion of lithium-ion in both electrolytes and cathode material, indicating sufficient mobility of lithium ions is required to maintain electrochemical performance of batteries.

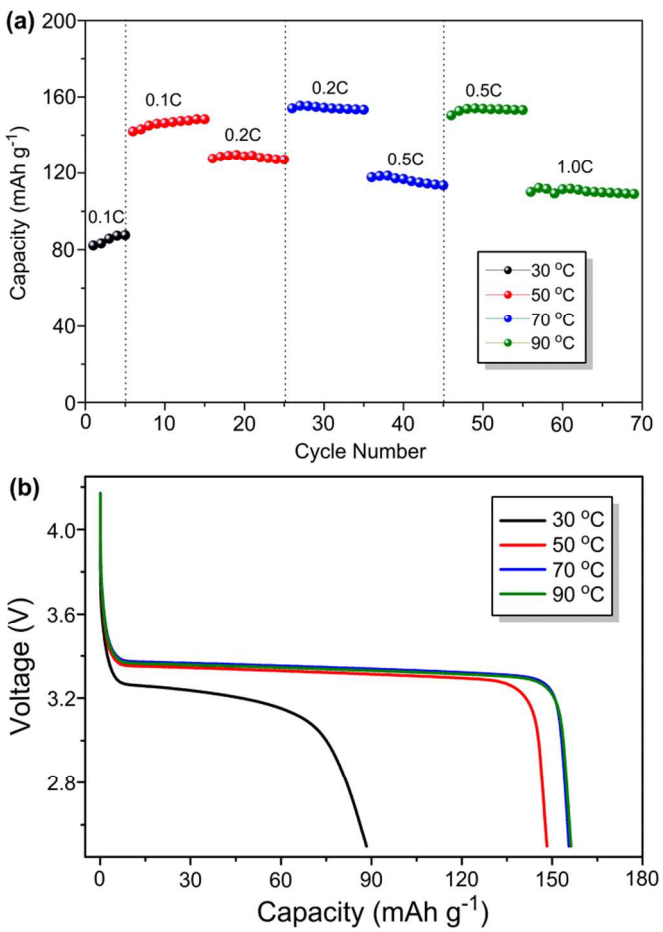

Fig. 7 (a) Discharge capacity at various temperatures and C-rates for $LiFePO_4$/HI-2/Li Cells, (b) representative discharge profile under different temperatures for $LiFePO_4$/HI-2/Li cells cycled under 0.1C charge-0.1C discharge conditions

The cycling stability of the cells at 90 °C was evaluated further through measurement of discharge capacity. The cells were charged at a current density of 0.2 C and discharged at a 0.5 C. Fig. 8 shows the cycling performance of cell made with our hybrid ionogels and the discharge profiles at various cycles (Fig. 8 inset), in comparison with the cells made with a well-known organic crosslinker, ETPTA-based ionogel.[44] The structure of ETPTA is shown in ESI, Fig S4†. The cells containing HI-2 ionogels exhibited relatively stable cycling performance. In addition, the discharge capacities for HI-2 were comparable to cells containing the liquid 1M LiTFSI BMPTFSI. (ESI, Fig S5†) The discharge capacity was able to maintain a value of 147.1 mAh g^{-1} after 50 cycles, which was 94.9% of its largest discharge capacity and the columbic efficiency of the system was found above 98% with the exception of cell activation. Moreover, no obvious change in the charge/discharge profiles or significant capacity decay were observed, confirming the thermal stability and electrochemical stability of the ionogels. In comparison, the cells containing organic crosslinker ETPTA-based ionogel exhibited a rapid capacity loss over repeatable cycling process and the discharge capacity decreased to 118.7 mA g^{-1}. That is a capacity retention of 82.7%, the greatest discharge capacity after being cycled merely for 50 times. It should be noted that HI-2 was able to fully solidify the ionic liquid at a mere 2 wt %, whereas the organic ionogel fabricated with ETPTA required a high concentration of cross-linker (15 wt %), which caused the significantly lower ionic conductivity compared with HI-2. (Fig. 4) Therefore, the improved electrochemical performances of the cell with ionogels could be ascribed to the less dense network-structure formed by LPMASQ, which could help to minimize the depreciation of the lithium-ion diffusion of the gel polymer electrolyte, resulting in enhanced electrochemical performances.

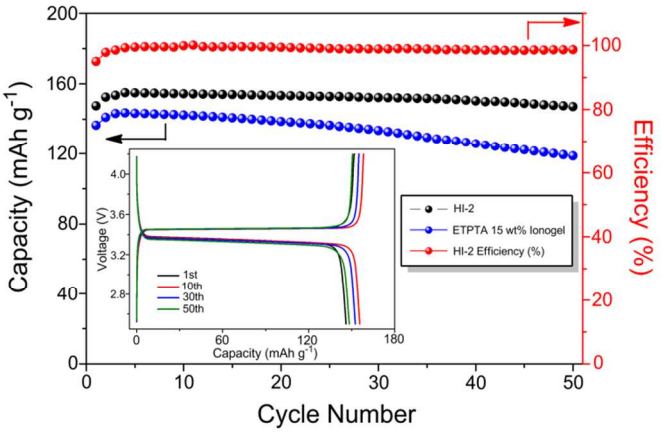

Fig. 8 Cyclability of HI-2 compared with a conventional organic ionogel fabricated with ETPTA, with the inset figure showing the representative discharge profiles for HI-2

Conclusions

Inorganic-organic hybrid ionogels were fabricated from a thermally curable (LPMASQ) as high temperature gel polymer electrolytes in Li batteries. Using an extremely simple mix and cure system, these hybrid ionogels exhibited thermal stability beyond 400 °C, stable mechanical properties at high temperatures and ionic conductivities on par with the neat ionic liquid. Li battery cell tests revealed that these hybrid ionogels could deliver high specific capacity and good cycling performance at elevated temperature, demonstrating the possible application of hybrid ionogels for Li batteries.

Acknowledgements

This work was financially supported by a grant from the Fundamental R&D Program for Core Technology of Materials and the Industrial Strategic Technology Development Program funded by the Ministry of Knowledge Economy, Republic of Korea, and partially by a grant from Centre for Materials Architecting of Korea Institute of Science and Technology (KIST).

Notes and references

[a] *Centre for Materials Architecturing, Korea Institute of Science and Technology, Hwarangno 14-gil 5, Seong-Buk Gu, Seoul 136-791, Republic of Korea*

[b] *Department of Chemical and Biological Engineering, and Institute of Chemical Process, Seoul National University, 599 Gwanak-ro, Gwanak-gu, Seoul 151-744, Republic of Korea*
[c] *Nanomaterials Science and Engineering, University of Science and Technology, 217 Gajungro, 176 Gajung-dong, Yuseong-Gu, Daejeon 305-333, Republic of Korea*

† Electronic Supplementary Information (ESI) available: [^{1}H NMR spectrum for BMPTFSI, interfacial resistance as a function of time, cyclic voltammogram, chemical structure of ETPTA, and representative discharge profiles for reference cells]. See DOI: 10.1039/b000000x/
‡ These authors contributed equally.

References

1. M. Armand, F. Endres, D. R. MacFarlane, H. Ohno and B. Scrosati, *Nature Mater.*, 2009, **8**, 621–629.
2. Y.-M. Chiang, *Science*, 2010, **330**, 1485–1486.
3. K. Xu, *Chem. Rev.*, 2004, **104**, 4303–4417.
4. Z. Chen, Y. Ren, A.N. Jansen, C.-K. Lin, W. Wang and K. Amine, *Nature Comm.*, 2013, **4**:1513.
5. J.-M. Tarascon and M. Armand, *Nature*, 2001, **414**, 359–367.
6. N.-S. Choi, Z. Chen, S.A. Frruenberger, X. Ji, Y.-K. Sun, K. Amine, G. Yushin, L.F. Nazar, J. Cho and P.G. Bruce, *Angew. Chem. Int. Ed*., 2012, **51**, 9994–10024.
7. A. Yoshino, *Angew. Chem. Int. Ed*., 2012, **51**, 5798–5800.
8. J. Y. Song, Y. Y. Wang and C. C. Wan, *J. Power Sources*, 1999, **77**, 183–197.
9. A. M. Stephan, *Eur. Polym. J.*, 2006, **42**, 21–42.
10. A. M. Stephan and K. S. Nahm, *Polymer*, 2006, **47**, 5952–5964.
11. M.P. Singh, R.K. Singh, and S. Chandra, *Prog. Mater. Sci.*, 2014, **64**, 73-120.
12. D. M. Tigelaar, M. A. B. Meador and W. R. Bennet, *Macromolecules*, 2007, **40**, 4159–4164.
13. A. I. Horowitz and M. J. Panzer, *J. Mater. Chem.*, 2012, **22**, 16534–16539.
14. A. K. Gupta, M. P. Singh, R. K. Singh and S. Chandra, *Dalton Trans.*, 2012, **41**, 6362–6371.
15. L. Viau, M.-A. Neouze, C. Biolley, S. Wolland, D. Brevet, P. Gaveau, P. Diudonne, A. Galarneau and A. Vioux, *Chem. Mater.*, 2012, **24**, 3128–3134.
16. F. Gayet, L. Viau, F. Leroux, S. Monge, J.-J. Robin and A. Vioux, *J. Mater. Chem.*, 2010, **20**, 9456–9462.
17. M.-A. Neouze, J.L. Bideau, P. Gaveau, S. Bellayer and A. Vioux, *Chem. Mater.*, 2006, **18**, 3931–3936.
18. T. Echelmeyer, H. W. Meyer and L. Wullen, *Chem. Mater.*, 2009, **21**, 2280–2285.
19. K. Matsumoto and T. Endo, *Macromolecules*, 2009, **42**, 4580–4584.
20. R. K. Donato, L. Matejka, H. S. Schrekker, J. Plestil, A. Jigounov, J. Brus and M. Slouf, J. Mater. Chem., 2011, 21, 13801–13810.
21. F. Gayet, L. Viau, F. Leroux, F. Mabille, S. Monge, J.-J. Robin and A. Vioux, *Chem. Mater.*, 2009, **21**, 5575–5577.
22. A. Vioux, L. Viau, S. Volland and J. L. Bideau, *C.R. Chimie*, 2010, **13**, 242–255.
23. M. Popall, M. Andrei, J. Kappel, J. Kron, K. Olma and B. Olsowski, *Electrochim. Acta*, 1998, **43**, 1155–1161.
24. Y. Lu, K. Korf, Y. Kambe, Z. Tu and L. A. Archer, *Angew. Chem. Int. Ed.*, 2014, **53**, 488–492.
25. J. L. Schaefer, D. A. Yanga and L. A. Archer, *Chem. Mater.*, 2013, **25**, 834–839.
26. Y. Lu, S. S. Moganty, J. L. Schaefer and L. A. Archer, *J. Mater. Chem.*, 2012, **22**, 4066–4072.
27. S. S. Moganty, S. Srivastava, Y. Lu, J. L. Schaefer, S. A. Rizvi and L.A. Archer, *Chem. Mater.*, 2012, **24**, 1386–1392.
28. S. K. Das, S. S. Mandal and A. J. Bhattacharyya, *Energy Environ. Sci.*, 2011, **4**, 139101399.
29. M. Patel, M. Gnanavel and A. J. Bhattacharyya, *J. Mater. Chem.*, 2011, **21**, 17419–17424.
30. S. K. Das and A. J. Bhattacharyya, *J. Phys. Chem. C.*, 2009, **16**, 6699–6705.
31. C. Pfaffenhuber, M. Gobel, J. Popovic and J. Maier, *Phys. Chem. Chem. Phys.*, 2013, **15**, 18318–18335.
32. R. H. Baney, M. Itoh, A. Sakakibara and T. Suzuki, *Chem. Rev.*, 1995, **95**, 1409–1430.
33. M. Li, W. Ren, Y. Zhang and Y. Zhang, *J. Appl. Polym. Sci.*, 2012, **126**, 273–279.
34. S.-J. Kwon, D.-G. Kim, J. Shim, J. H. Hong, J.-H. Baik and J-C. Lee, *Polymer*, 2014, **12**, 2799–2808.
35. J. Shim, D.-G. Kim, J. H. Lee, J. H. Baik and J.-C. Lee, *Polym. Chem.*, 2014, **5**, 3432–3442.
36. D.-G. Kim, J. Shim, J. H. Lee, S.-J. Kwon, J.-H. Baik and J.-C. Lee, *Polymer*, 2013, **21**, 2812–5820.
37. A. S. Lee, J. H. Lee, J.-C. Lee, S. M. Hong, S. S. Hwang and C. M. Koo, *J. Mater. Chem. A.*, 2014, **2**, 1277–1283.
38. A. S. Lee, S. S. Choi, H. S. Lee, H. Y. Jeon, K. Y. Baek and S. S. Hwang, *J. Polym. Sci. Part A: Polym. Chem.*, 2012, **50**, 4563–4570.
39. S. S. Choi, A. S. Lee, H. S. Lee, H. Y. Jeon, K. Y. Baek and S. S. Hwang, *J. Polym. Sci. Part A: Polym. Chem.*, 2011, **49**, 5012–5018.
40. S. S. Choi, H. S. Lee, S. S. Hwang, D. H. Choi and K. Y. Baek, *J. Mater. Chem.*, 2010, **20**, 9852–9854.
41. Z. X. Zhang, J. Hao, P. Xie, X. Zhang, C. C. Han and R. Zhang, *Chem Mater.*, 2008, **20**, 1322–1330.
42. S. Chang, T. Matsumoto, H. Matsumoto and M. Unno, *Appl. Organometal. Chem.*, 2010, **24**, 241–246.
43. Z-B. Zhou, H. Matsumoto and K. Tatsumi, *Chem. Eur. J.* 2006, **12**, 2196–2212.
44. S.-H. Kim, K.–H. Choi, S.-J Cho, E.-H. Kil and S.–Y. Lee, *J. Mater. Chem. A*, 2013, **1**, 4949–4955.
45. M. A. Navarra, J. Manzi, L. Lombardo, S. Panero and B. Scrosati, *ChemSusChem*., 2011, **4**, 125–130.
46. V. Gentili, S. Panero, P. Reale and B. Scrosati, *J. Power Source*, **170**, 2007, 185–190.
47. M. Wetjen, M. A. Navarra, S. Panero, S. Passerini, B. Scrosati and J. Hassoun, *ChemSusChem*., **6**, 2013, 1037–1043.
48. L.-X. Yuan, Z.-H. Wang, W.-X. Zhang, X.-L. Hu, J.-T. Chen, Y.-H. Huang and J. B. Goodenough, *Energy Environ. Sci*., 2011, **4**, 269–284.

